ELSEVIER

Preparation of CdS-containing silica–titania composites by the sol–gel process

Vilma C. Costa [a],[*], Fernando S. Lameiras [a], Maria Terezinha C. Sansviero [b], A.B. Simões [c], W.L. Vasconcelos [c]

[a] *Centro de Desenvolvimento da Tecnologia Nuclear, Rua Mário Werneck, s/n, Campus-Pampulha, Belo Horizonte/MG, CP 941, CEP: 30123-970, Brazil*
[b] *Department of Chemistry, ICEx, UFMG, BH, MG CEP 31270-901, Brazil*
[c] *Department of Metallurgical and Materials Engineering, UFMG, Rua Espírito Santo, 35, s/206, BH, MG, CEP: 30160-030, Brazil*

Abstract

Silica–titania composite materials containing 20 mol% TiO_2 were prepared by sol–gel process using tetraethoxysilane (TEOS) and titanium isopropoxide $(Ti(OPr)_4)$ as precursors. A two-stage hydrolysis procedure was performed in acid conditions for preparation of the TiO_2–SiO_2 oxides. Nanometer sized crystallites of CdS were incorporated into TiO_2–SiO_2 matrices by complex formation with thiourea, $SC(NH_2)_2$. The influence of the preparation route and calcination temperature on the structural characteristics and physico-chemical properties of TiO_2–SiO_2 and CdS/TiO_2–SiO_2 materials was studied by means of nitrogen physisorption, X-ray diffraction, infrared spectroscopy and atomic force microscopy. The results indicate that anatase phase is stable at temperatures up to 600 °C for TiO_2–SiO_2 matrices and the addition of CdS particles affects the system crystallization.
© 2004 Published by Elsevier B.V.

1. Introduction

Titania–silica materials are of great importance as glasses especially in applications as advanced materials [1,2], catalysts [3], and support for acid-catalyzed [4–6] and selective oxidation reactions [7,8].

Methods of preparation that allow molecular-scale mixing of the constituents with a high degree of homogeneity are advantageous. The resulting porosity and homogeneity at atomic level of titania–silica mixed oxides have been associated to differences in the synthesis preparation [9].

A number of methods have been applied to fabricate TiO_2–SiO_2 composites including coprecipitation [6], flame hydrolysis [10], and sol–gel route [11,12]. It has been associated to the sol–gel synthesis controllable morphology and particle size of the final product through varying experimental conditions [13].

TiO_2 as a photocatalyst is active in the UV region and is considered a very promising catalyst for removal of air and water contaminants. Rutile and anatase crystalline phases of titania are used in photocatalysis [3], with anatase showing higher photocatalytic activity. One of the limiting factors that is associated with the efficiency of photocatalysis is the fast recombination of charge carriers in the system. To overcome this problem, it has been suggested [14–16] that the coupling of semiconductors with appropriate energy levels can produce a more efficient photocatalyst via better charge separation. Such coupled semiconductors are potentially useful in improving the photocatalytic conversion efficiency of photoelectrochemical systems. It seems crucial to

---

investigate ways of developing dispersed porous materials with distributed stabilized semiconductor nanoparticles.

In order to understand the structural characteristics and the relationships with the physico-chemical properties of those systems we report the preparation of TiO_2–SiO_2 and CdS/TiO_2–SiO_2 composites using two different hydrolysis routes. The similarities and differences in structural characteristics and properties are discussed.

2. Experimental

2.1. Sample preparation

The SiO_2–TiO_2 solutions were prepared, basically, following the literature procedure [17], using tetraethoxysilane (TEOS) and titanium isopropoxide (TIP) as precursors. We have prepared two groups of undoped SiO_2–TiO_2 and CdS-contained mixed oxides in the composition $80SiO_2$–$20TiO_2$ mol%. In the first synthesis procedure, TEOS was first partially hydrolyzed in a mixed solution of H_2O, C_2H_5OH (TEOS/EtOH/H_2O = 1/4/2) and enough HCl to achieve an initial solution pH of 1.5. After the solution was stirred for 1 h, acetic acid was added to the initial solution (TIP/HAc = 1/10) and then titanium isopropoxide, $Ti(OC_3H_7)_4$, was dropwised into the prepared solution. Water was added to complete molar ratio of alkoxide/H_2O = 1/4. For identification purpose in this work, samples prepared by this procedure are labeled with the prefix SA.

In the second procedure, TEOS was mixed with ethanol, water and HCl (TEOS/EtOH/ H_2O = 1/4/2). In a separate container, titanium isopropoxide was mixed with 2-etoxyethanol and acetic acid in the molar ratio TIP/2-etoxyethanol/HAc = 1/8/10 during 10 min. The TEOS prehydrolysis solution was allowed to stir for 30 min, and after that the two solutions were mixed together. Samples prepared by this procedure were labeled with the prefix ST.

For the doped CdS/SiO_2–TiO_2 samples, an intermediate step was done. Cadmium acetate, $Cd(OAc)_2 \cdot 2H_2O$, and thiourea, $SC(NH_2)_2$, in a molar ratio of 1/2, were previously dissolved in CH_3OH (TEOS/MeOH = 1/5). A molar ratio Cd/(Si+Ti) = 0.01 and 0.03 was used. In both procedures, the methanol solution was added to the TEOS solution before adding titanium isopropoxide.

After stirring, the sols were cast into plastic vials. After gelation, the samples were aged at 60 °C for 2 days and then dried at 90 °C for 2 days. The gels were first heated to 300 °C and 600 °C in air for 10 h. Doped SiO_2–TiO_2 gels were heated to 300 °C to avoid oxidation of resultant CdS and also the evaporation of sulfur during the heat treatment. Table 1 presents the sample labels, composition (mol%), and heat treatment of the gels.

2.2. Measurements

The FTIR transmission spectra were measured using a spectrophotometer (Bomem model 102) by the KBr pellet method.

The crystalline structures of the phases in the samples was characterized with X-ray powder diffraction, using a Rigaku equipment, with CuK_α ($\lambda = 1.5418$ Å) incident radiation over 2θ range of 10–70°.

Nitrogen adsorption–desorption experiments were performed at 77 K using a Quantachrome equipment, model Nova 2200.

The morphology of samples was investigated using tapping-mode atomic force microscopy imaging (AFM), using a Shimadzu Scanning Probe microscope, SPM9500-J3.

3. Results and discussion

3.1. Nitrogen physisorption

The specific surface area (S_{BET}), total pore volume (V_p), and mean pore diameter (D_p) for the SiO_2–TiO_2

Table 1
Nominal composition (mol%), heat treatment conditions, and structural properties of the gels

Label	SiO_2	TiO_2	Cd/(Si + Ti) molar ratio	Treatment (°C)	Surface area (m²/g)	V_p (cm³/g)	D_p (Å)
ST	80	20	–	110	870 ± 43	0.69 ± 0.03	32.0 ± 1.6
SA	80	20	–	110	571 ± 28	0.37 ± 0.02	25.7 ± 1.3
ST-th2	80	20	0.03	110	540 ± 27	0.41 ± 0.02	30.4 ± 1.5
SA-th2	80	20	0.03	110	651 ± 33	0.42 ± 0.02	25.6 ± 1.3
SA-th3	80	20	0.01	110	549 ± 27	0.33 ± 0.02	24.1 ± 1.2
ST	80	20	–	300	666 ± 33	0.52 ± 0.03	31.0 ± 1.6
SA	80	20	–	300	463 ± 23	0.29 ± 0.01	25.3 ± 1.3
ST-th2	80	20	0.03	300	686 ± 34	0.41 ± 0.02	23.8 ± 1.2
SA-th2	80	20	0.03	300	551 ± 28	0.33 ± 0.02	23.8 ± 1.2
SA-th3	80	20	0.01	300	563 ± 28	0.33 ± 0.02	23.7 ± 1.2
ST	80	20	–	600	388 ± 19	0.32 ± 0.02	33.4 ± 1.7
SA	80	20	–	600	374 ± 19	0.28 ± 0.01	29.5 ± 1.5

mixed oxide and CdS/SiO_2–TiO_2 doped samples, heated at 110 °C, 300 °C, and 600 °C are presented in Table 1. All samples presented high surface areas and pores in the mesopore range. For samples prepared with the ST synthesis procedure, usually, the mean pore diameter is bigger, but slightly reduced in size with CdS doping.

There is a tendency of reducing the specific surface area when the temperature of the heat treatment changes from 110 °C to 600 °C for samples prepared by both procedures, but the total pore volume and the mean pore diameter seems to be less affected. At 600 °C a significant decline of surface areas was observed with both procedures for the undoped composition. The surface area and porosity of the ST procedure samples indicate a dependence on the type of prehydrolysis route chosen. Also, the increase of the surface area for doped samples, after heating in air at 300 °C, could be a result of the removal of the organic residues, rendering the surface accessible for physisorption of nitrogen.

3.2. X-ray diffraction

The diffractograms taken on SiO_2–TiO_2 oxides powder samples are reported in Figs. 1 and 2. Fig. 1 shows XRD spectra for samples prepared from procedure SA, for the compositions undoped and doped with CdS and Fig. 2 for samples prepared from synthesis procedure ST.

In the sol–gel SiO2/TiO2 undoped system, crystalline anatase phase is stable at 300 °C and 600 °C in amorphous silica phase, for both synthesis procedures used. All the peaks of the XRD pattern were found to be indexed to anatase phase [12]. The size of anatase nanocrystals was estimated using the well-known Scherrer equation and considering the (101) reflection line ($2\theta = 25.6$). For undoped sample from synthesis SA
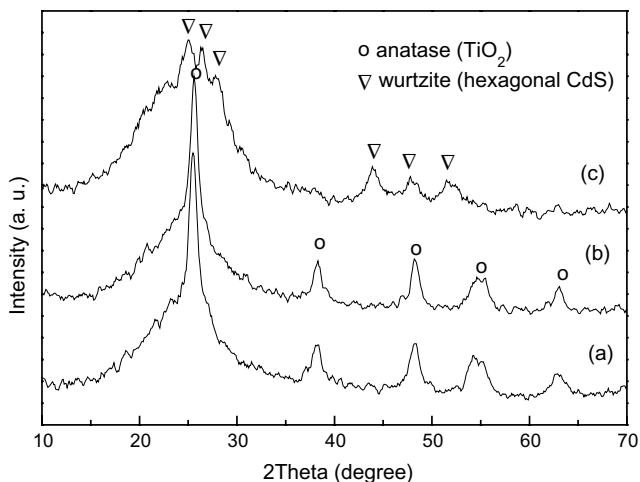

Fig. 1. X-ray diffraction pattern for samples prepared by procedure SA: (a) SA sample heated at 300 °C, (b) SA sample heated at 600 °C, (c) SA-th2 doped sample heated at 300 °C.
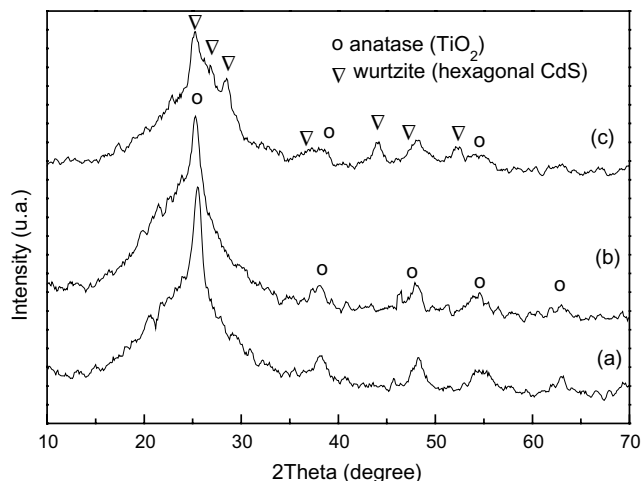

Fig. 2. X-ray diffraction pattern for samples prepared by procedure ST: (a) ST sample heated at 300 °C, (b) ST sample heated at 600 °C, (c) ST-th2 doped sample heated at 300 °C.

(Fig. 1), heated to 300 °C, the calculated size is 7.2 nm and for sample heated to 600 °C is 7.4 nm. The calculated average size of anatase crystallites for undoped sample from synthesis ST (Fig. 2), heated to 300 °C, is 5.9 nm and for sample heated to 600 °C is 7.4 nm.

From Fig. 1 (SA synthesis procedure), it can be seen for the CdS doped sample, heated at 300 °C, that crystals of CdS are present as hexagonal wurtzite type structure and peaks corresponding to anatase phase present in the undoped sample of same composition are no longer seen. The results from X-ray also indicate that the presence of CdS crystals might inhibit nucleation of anatase phase or keep the particles from growing larger.

From Fig. 2 (ST synthesis procedure), for the doped composition of the mixed oxide, peaks characteristics of anatase are still present along with the hexagonal phase of CdS crystals. The corresponding anatase peaks have a very low intensity.

3.3. Atomic force microscopy

To examine the morphology of the samples on a nanometer scale, we have used tapping-mode atomic force microscopy (AFM). Two images were selected to be shown for samples doped with CdS treated at 300 °C.

The AFM images show distinct particles and aggregates. Fig. 3 shows the morphology for sample SA-th2 ($80SiO_2$–$20TiO_2$/CdS) heated at 300 °C. This image reveals that particles are homogeneous in size and distribution. From this image and the X-ray diffraction studies, we suspect that this structure results from mixed SiO_2–TiO_2 oxide, since no peaks related to TiO_2 crystals could be seen, but only hexagonal CdS nanocrystals. On the other hand, for sample ST-th2 ($80SiO_2$–$20TiO_2$/CdS) heated at 300 °C, (Fig. 4), the AFM image shows very
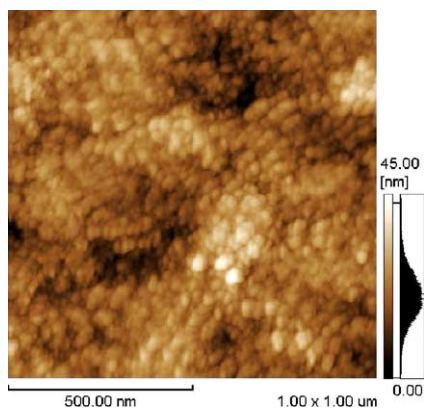
Fig. 3. Tapping-mode AFM image for sample SA-th2 (80SiO$_2$–20TiO$_2$/CdS) heated at 300 °C.
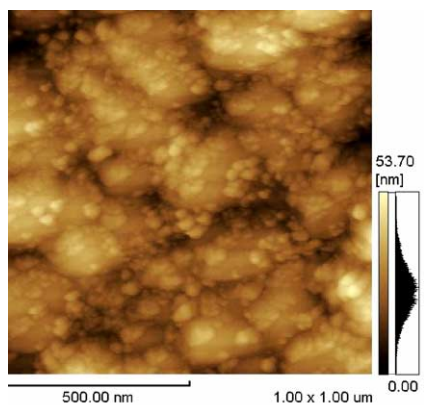

Fig. 4. Tapping-mode AFM image for sample ST-th2 (80SiO$_2$–20TiO$_2$/CdS) heated at 300 °C.

small particles spread over coalesced particles. The XRD results for this sample showed that the crystalline phase formed consisted of anatase and hexagonal CdS. The weaker peaks found for anatase might be an indication that Ti is presented as nanoparticles. From these observations, we suggest that the formation of CdS crystals affects the crystallization of sol–gel derived SiO$_2$–TiO$_2$ by stabilizing the amorphous region for samples prepared by SA procedure, and changing the size and aggregation of the TiO$_2$ phase formed for samples prepared by the ST procedure.

3.4. FTIR Spectroscopy

The FTIR spectra of the sol–gel SiO$_2$–TiO$_2$ samples heated at 110 °C and 300 °C are shown in Fig. 5(a) and (b). The vibrational modes due to Si–O–Si asymmetric stretching are observed at approximately 1070 cm^{-1} and 1200 cm^{-1}. Those peaks correspond respectively to transversal optical and longitudinal optical modes [12,18]. Additional peaks are seen at 790 cm^{-1} for symmetric Si–O–Si stretching vibration [19], and at
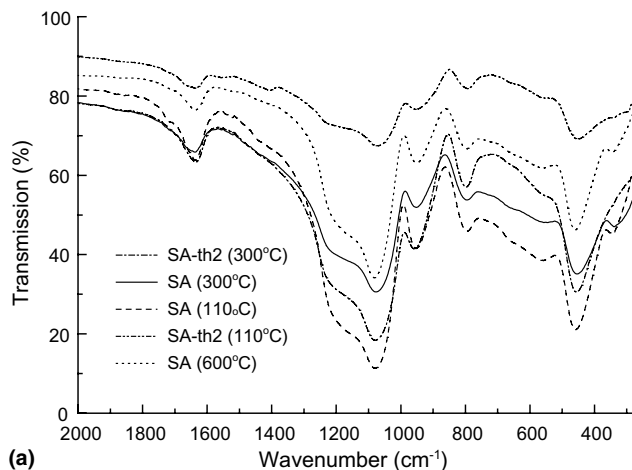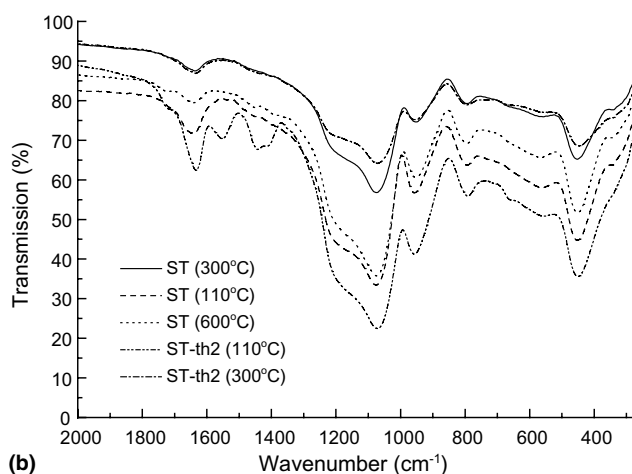
Fig. 5. FTIR spectra of sol–gel TiO$_2$–SiO$_2$ samples: (a) samples prepared by synthesis procedure SA; (b) samples prepared by synthesis procedure ST. The spectrum label for each sample is indicated on the figure.

450 cm^{-1} (for Si–O–Si bending modes). A typical absorption band observed in silica gel is located at 1640 cm^{-1} and is attributed to a deformation mode of adsorbed molecular water in the pores. The band at ca. 950 cm^{-1} is assigned to a Si–O–Ti stretching [12,20]. This band has been ascribed to a vibration involving SiO$_4$ tetrahedra bonded to a four-fold coordinated titanium atom and indicates a good mixing of Ti and Si at atomic level [21]. This feature also has been assigned to the stretching vibration of silanol groups in pure silica [22]. In this way, the band located around 950 cm^{-1}, in our work, could be a superimposed band with coupled vibrational modes of Si–O$^-$ stretching and Si–O–Ti linkages. The dispersion of Ti in SiO$_2$ matrix has been usually [12] associated with the ratio of infrared vibration due to Ti–O–Si band at 930–960 cm^{-1} to that due to Si–O–Si at ca 1200 cm^{-1}.

The spectra of doped samples, SA-th2 and ST-th2, heated at 110 °C show additional peaks located at 1550 cm^{-1}, 1442 cm^{-1} and 1412 cm^{-1}. Those are assigned

to organic groups. The FTIR spectrum of thiourea shows the same peaks [23]. These bands disappear as temperature increases to 600 °C.

4. Conclusions

Silica–titania composites have been prepared by the sol–gel method. Nanocrystalline anatase phase is stable after annealing the samples up to 600 °C. The addition of CdS particles affects the crystallization of sol–gel derived SiO_2–TiO_2 by stabilizing amorphous phase. Different preparation methods and synthesis conditions influence the homogeneity of the component mixture at the nanometric level. Therefore, to develop a fundamental understanding about the catalysis and chemistry of these materials, the investigation of the oxidation states of Ti atoms in silica–titania/CdS system is under investigation.

Acknowledgments

References

[1] D. Zhu, T. Kosugi, J. Non-Cryst. Solids. 202 (1996) 88.
[2] S. Satoch, K. Susa, I. Matsuyama, J. Non-Cryst. Solids 146 (1992) 121.
[3] V. Lafond, P.H. Mutin, A. Vioux, J. Mol. Catal. A 182 (2002) 81.
[4] M. Itoh, H. Hattori, K. Tanabe, J. Catal. 35 (1974) 225.
[5] E.I. Ko, J.P. Chen, J.G. Weisman, J. Catal. 105 (1987) 511.
[6] J.R. Sohn, H.J. Jang, J. Catal. 132 (1991) 563.
[7] R. Neumann, M. Chava, M. Levin, J. Chem. Soc. Commun. 1685 (1993).
[8] B. Notari, Catal. Today 18 (1993) 163.
[9] J.B. Miller, S.T. Jonhston, E.I. Ko, J. Catal. 150 (1994) 311.
[10] M. Kawachi, M. Yasu, T. Edahiro, Electron. Lett. 19 (1983) 583.
[11] R.R.A. Syms, A.S. Holms, J. Non-Cryst. Solids. 170 (1994) 223.
[12] D.C.M. Dutoit, M. Schneider, A. Baiker, J. Catal. 153 (1995) 165.
[13] E. Scolan, C. Sanchez, Chem. Mater. 10 (1998) 3217.
[14] L. Spanghel, H. Weller, A. Henglein, J. Am. Chem. Soc. 109 (1987) 6632.
[15] S. Hotchandani, P.V. Kamat, J. Phys. Chem. 96 (1992) 6834.
[16] P.A. Sant, P.V. Kamat, Phys. Chem. Chem. Phys. 4 (2002) 198.
[17] R.F.S. Lenza, PhD dissertation, UFMG, 2000.
[18] R.M. Almeida, C.G. Pantano, J. Appl. Phys. 68 (1990) 4225.
[19] A. Bertoluzzi, C. Fagnano, M.A. Morelli, V. Gottardi, M. Guglielmi, J. Non-Cryst. Solids 48 (1982) 117.
[20] I.M.M. Salvado, J.M.F. Navarro, J. Non-Cryst. Solids 147&148 (1992) 256.
[21] M. Beghi, P. Chiurlo, L. Costa, M. Palladino, M.F. Pirini, J. Non-Cryst. Solids 145 (1992) 175.
[22] M. Aizawa, Y. Nosaka, N. Fuji, J. Non-Cryst. Solids 168 (1994) 49.
[23] N. Tohge, M. Asuka, T. Minami, SPIE, Sol–Gel Opt. 1328 (1990) 125.